Wind and Structures, Vol. 15, No. 5 (2012) 409-421
DOI: http://dx.doi.org/10.12989/was.2012.15.5.409

Verification of a tree canopy model and an example of its application in wind environment optimization

Yi Yang*[1,2], Zhuangning Xie[1], Tim K.T. Tse[2], Xinyang Jin[3] and Ming Gu[4]

[1]*State Key Laboratory of Subtropical Building Science, South China University of Technology, Guangzhou, China*
[2]*Department of Civil and Environmental Engineering, The Hong Kong University of Science and Technology, Clear Water Bay, Kowloon, Hong Kong, China*
[3]*Center of Wind Engineering Research, China Academy of Building Research, Beijing, China*
[4]*State Key Laboratory for Disaster Reduction in Civil Engineering, Tongji University, Shanghai, China*

(Received February 24, 2011, Revised June 1, 2011, Accepted October 16, 2011)

Abstract. In this paper, the method of introducing additional source/sink terms in the turbulence and momentum transport equations was applied to appropriately model the effect of the tree canopy. At first, the new additional source term for the turbulence frequency ω equation in the SST k-ω model was proposed through theoretical analogy. Then the new source/sink term model for the SST k-ω model was numerically verified. At last, the proposed source term model was adopted in the wind environment optimal design of the twin high-rise buildings of CABR (China Academy of Building Research). Based on the numerical simulations, the technical measure to ameliorate the wind environment was proposed. Using the new inflow boundary conditions developed in the previous studies, it was concluded that the theoretically reasonable source term model of the SST k-ω model was applicable for modeling the tree canopy flow and accurate numerical results are obtained.

Keywords: wind environment; high-rise building; numerical simulation; SST k-ω model; additional source/sink term; optimization design

1. Introduction

In studies on wind environment around buildings, usually the influence of vegetation cover cannot be ignored. The windbreak formed by the vegetation cover increases the wind drag and subsequently reduces the downstream wind speed effectively. Vegetation cover and its influences on surface roughness have therefore induced considerable complexity to computational modeling of airflow.

For large-scale atmospheric flows, the broad characteristics of flow are concerned more, and the modified wall function considering roughness modification can be then used to model the near ground flow. From the viewpoint of numerical simulation, the wall function has substantially reduced the excessive grid requirement, particularly in the viscous sub-layer. It is however that this method is not suitable for modeling the near ground canopy flow since the use of roughness parameters in the modified law of the wall provides no information of the turbulence structure

* Corresponding author, Dr., E-mail: yiyangbox@163.com

within the canopy region in terms of the vegetation-related parameters, such as leaf area density (LAD) (Pattanapol *et al*. 2008).

In focusing on surface flow complexity, plant drag can be accounted for by incorporating surface roughness parameters and/or introducing additional source/sink terms (Svensson *et al*. 1990, Green 1992, Liu *et al*. 1996, Pattanapol *et al*. 2008). As such, modified transport equations can be derived to establish mean momentum, turbulent kinetic energy and turbulent kinetic dissipation rate.

In this paper, a more appropriate source term S_ω in the k-ω model has been deduced through the theoretical analogy with the two turbulence models, i.e., the k-ω model and the k-ω model. The new source term S_ω for the SST k-ω model was numerically verified by comparing the numerical results with the mean velocity profiles at different downstream locations of the vegetated windbreak experiment conducted by Kurotani *et al*. (2002). At last, the proposed source term model was adopted in the wind environment optimal design of the twin high-rise buildings of China Academy of Building Research (CABR). The effects of tree canopy on the wind flow in the passage formed by the two closely arranged buildings was numerically investigated and then compared with the situation without the tree canopy. In the numerical simulations, the new inflow boundary conditions proposed by Yang *et al*. (2008, 2009a, b) are used to model the equilibrium atmospheric boundary layer (ABL). By using these new inflow boundary condition profiles, the streamwise errors can be significantly reduced if a good fit between the inflow profiles and the model is used (O'Sullivan 2011). Based on the results of the numerical simulation, technical measures to ameliorate the unfavorable wind environment were then suggested.

2. Turbulence models and additional source/sink terms

2.1 Standard k-ε model

The continuity and momentum equations for an incompressible flow are given below

$$\frac{\partial u_i}{\partial x_i} = 0 \tag{1}$$

$$\frac{\partial u_i}{\partial t} + \frac{\partial u_i u_j}{\partial x_j} = -\frac{\partial p}{\partial x_i} + \frac{\partial}{\partial x_j}\left[v_t\left(\frac{\partial u_i}{\partial x_j} + \frac{\partial u_j}{\partial x_i}\right) - \frac{2}{3}\delta_{ij}k\right] + S_{ui} \tag{2}$$

For the standard k-ε model, the governing equations for the turbulent kinetic energy k and its dissipation rate ε can be expressed as follows

$$\frac{\partial k}{\partial t} + \frac{\partial u_i k}{\partial x_i} = \frac{\partial}{\partial x_j}\left(\frac{v_t}{\sigma_k}\frac{\partial k}{\partial x_j}\right) + P_k - \varepsilon + S_k \tag{3}$$

$$\frac{\partial \varepsilon}{\partial t} + \frac{\partial u_i \varepsilon}{\partial x_i} = \frac{\partial}{\partial x_j}\left(\frac{v_t}{\sigma_\varepsilon}\frac{\partial \varepsilon}{\partial x_j}\right) + \frac{\varepsilon}{k}(C_{1\varepsilon}P_k - C_{2\varepsilon}\varepsilon) + S_\varepsilon \tag{4}$$

where k and ε are the turbulent kinetic energy and its dissipation rate, respectively, and P_k is the production of turbulent kinetic energy, which is expressed as

$$P_k = v_t\left(\frac{\partial u_i}{\partial x_j} + \frac{\partial u_j}{\partial x_i}\right)\frac{\partial u_i}{\partial x_j} \tag{5}$$

In Eqs. (2), (3) and (4), the S_{ui}, S_k and S_ε are the additional source/sink terms of the momentum, k and transport equations, respectively. The eddy viscosity in the standard *k-ε* model is given by

$$V_t = C_\mu \frac{k^2}{\varepsilon} \tag{6}$$

Eqs. (3), (4) and (6) contain five adjustable constants C_μ, σ_k, σ_ε, $C_{1\varepsilon}$ and $C_{2\varepsilon}$. Values of these constants have been obtained by comprehensive data fitting for a wide range of turbulent flows (Versteeg and Malalasekera 1995) and are listed below

$$C_\mu = 0.09,\ \sigma_k = 1.0,\ \sigma_\varepsilon = 1.3,\ C_{1\varepsilon} = 1.44,\ C_{2\varepsilon} = 1.92$$

2.2 k-ω model

For the *k-ω* model (Menter 1994), the governing equations for the turbulent kinetic energy *k* and turbulence frequency can be expressed as follows

$$\frac{\partial k}{\partial t} + \frac{\partial u_i k}{\partial x_i} = \frac{\partial}{\partial x_j}\left(\frac{v_t}{\sigma_k}\frac{\partial k}{\partial x_j}\right) + P_k - Y_k + S_k \tag{7}$$

$$\frac{\partial \omega}{\partial t} + \frac{\partial u_i \omega}{\partial x_i} = \frac{\partial}{\partial x_j}\left(\frac{v_t}{\sigma_\omega}\frac{\partial \omega}{\partial x_j}\right) + P_\omega - Y_\omega + S_\omega \tag{8}$$

where P_k and P_ω represents the production terms of *k* and *ω*, and Y_k and Y_ω are the effective dissipation terms due to turbulence. The S_k and S_ω are the additional source/sink terms of the *k* and transport equations, respectively. The turbulent viscosity is computed by combining *k* and *ω* as follows

$$v_t = \frac{k}{\omega} \tag{9}$$

2.3 Additional source/sink terms model of the SST k-ω model

The *k-ω* based SST model developed by Menter (1994) employs the *k-ω* model near the surface and the *k-ω* model in the free-shear layers. A blending function is adopted to bridge these two models. The SST *k-ω* model takes into account of the transport of the turbulent shear stress and gives accurate predictions of the onset and the amount of flow separation under adverse pressure gradients (Menter 1994). In view of its relatively high efficiency for numerical simulation and accurate solution, the SST *k-ω* model was adopted in this study.

The plant effects were accounted for by introducing the additional source/sink terms in the mean momentum, the turbulence kinetic energy k and turbulence frequency ω equations in the SST k-ω model, which is more suitable for blunt body flow, compared with the standard k-ε model (Yang *et al*. 2008). The expressions of the additional source/sink terms have been proposed by a number of researchers (e.g., Svensson *et al*. 1990, Green 1992, Liu J. *et al*. 1996). Mochida *et al*. (2006) conducted a numerical study and compared the performances of different forms of additional source/sink terms on the tree canopy flow.

For the k-ε model, the source/sink terms accounting for the plant drag are expressed as follows (Mochida *et al*. 2008)

$$S_{ui} = -C_d A u_i U \tag{10}$$

$$S_k = C_d A \beta_p U^3 - C_d A \beta_d U k \tag{11}$$

$$S_\varepsilon = C_d A \alpha_p \beta_p \frac{\varepsilon}{k} U^3 - C_d A \alpha_d \beta_d \frac{\varepsilon}{k} U k \tag{12}$$

In Eqs. (10), (11) and (12), C_d is the drag coefficient; A is the leaf area density (LAD) (m^2m^{-3}); u_i is the velocity component of i direction; where $U=|u_iu_i|^{1/2}$ is the absolute value of the spatially averaged wind speed. β_p was the fraction of mean flow kinetic energy being converted to wake-generated energy by canopy drag, and β_d was the magnitude of energy losses from interactions with obstacles. For the standard k-ε model, the typical values of β_p and β_d are 1 and 4, respectively (Sogachev and Panferov 2006). α_p and α_d are the adjustable model constants, and the analytical values are both 1.5. For the SST k-ε model, the values of α_p and α_d are modified to 3.2 and 0, respectively (Neary 2003, Pattanapol *et al*. 2008).

Due to the relationship between the SST k-ω model and the standard k-ε model, the source/sink terms of the mean momentum and k equations in the standard k-ε model, i.e., Eqs. (10) and (11), can be adopted in the SST k-ω model directly. While, for the source/sink term of the ω equation, almost no theoretical expression can be referred to directly. For example, Pattanapol *et al*. (2008) adopted the equation of S_ε as the form of the expression of S_ω directly only through a simple linear transformation between ε and ω.

In order to obtain a reasonable source term S_ω, a derivation was conducted. The detailed procedures are described as follows

(1) Given the relation of ε and ω, i.e., $\varepsilon = C_\mu \omega k$, and substitute into Eq. (4). Eq. (13) was obtained after an expansion and linear transformation operation

$$\frac{\partial k}{\partial t} + \frac{k}{\omega}\frac{\partial \omega}{\partial t} + \frac{\partial u_i k}{\partial x_i} = \frac{k}{\omega}\frac{\partial u_i \omega}{\partial x_i} = \frac{1}{\omega}\frac{\partial}{\partial x_j}\left[\frac{\nu_t}{\sigma_\varepsilon}\left(\omega\frac{\partial k}{\partial x_j} + k\frac{\partial \omega}{\partial x_j}\right)\right] + (C_{1\varepsilon}P_k - C_{2\varepsilon}\varepsilon) + \frac{S_\varepsilon}{C_\mu \omega} \tag{13}$$

(2) Subsequently, a combination of Eq.(13) with Eq. (3), would produce Eq. (14)

$$\frac{k}{\omega}\frac{\partial \omega}{\partial t} + \frac{k}{\omega}\frac{\partial u_i \omega}{\partial x_i} = \frac{1}{\omega}\frac{\partial}{\partial x_j}\left[\frac{\nu_t}{\sigma_\varepsilon}\left(\omega\frac{\partial k}{\partial x_j} + k\frac{\partial \omega}{\partial x_j}\right)\right] - \frac{\partial}{\partial x_j}\left(\frac{\nu_t}{\sigma_k}\frac{\partial k}{\partial x_j}\right) + (C_{1\varepsilon} - 1)P_k - (C_{2\varepsilon} - 1)\varepsilon + \frac{S_\varepsilon}{C_\mu \omega} - S_k \tag{14}$$

(3) Through analogy with Eq. (8), therefore, the relationship as expressed in Eq. (15) of the additional source/sink term for was obtained

$$S_\omega = \left(\frac{S_\varepsilon}{C_\mu \omega} - S_k\right)\frac{\omega}{k} \tag{15}$$

(4) Eq. (15) related the S_ω to S_k and S_ε. Substituting Eqs. (11) and (12) into Eq. (15), following equation can be obtained

$$\begin{aligned} S_\omega &= C_d A(\alpha_p - 1)\beta_p \frac{\varepsilon}{C_\mu k^2} U^3 - C_d A(\alpha_d - 1)\beta_d \frac{\varepsilon}{C_\mu k^2} Uk \\ &= C_d A(\alpha_p - 1)\beta_p \frac{\omega}{k} U^3 - C_d A(\alpha_d - 1)\beta_d \frac{\omega}{k} Uk \end{aligned} \tag{16}$$

The newly-derived source term S_ω of Eq. (16), which was deduced from the turbulence model equations, will be employed along with the source/sink terms of S_u and S_k in the numerical simulation of windbreak flow in the next section.

3. Numerical verification

3.1 Model Setup

Kurotani *et al*. (2002) performed a field experiment of vegetated windbreak flow and the experimental results are available in the website (http://www.aij.or.jp/). Based on the experimental results, Mochida *et al*. (2006) carried out a series of parameter optimization studies on the additional source/sink terms of k-ε model.

In this paper, the experiment and the numerical simulations conducted by Mochida *et al*. (2006) were referred to, and a corresponding 2D numerical model was built as shown in Fig. 1. The dimensions of the rectangular computational domain were 100 m(L) × 100 m(W), which could be referred to Franke *et al*. (2007). The domain was discretized by structural grids and the finest mesh grid close to the ground was set as 0.1 m. The total amount of cells was 50,000. The present work was conducted using the CFD code Fluent 6.3 (Fluent Inc.). The effect of tree canopy on the wind flow was modeled by adding the source/sink terms of S_u, S_k and S_ω (i.e., Eqs. (10), (11) and (16)) into the momentum, k and ω equations, respectively, using the user defined functions (UDF). The flow was assumed incompressible and steady, and the SIMPLE algorithm was used for pressure-velocity coupling. The second order upwind difference scheme, QUICK, was adopted for all the convective terms in the momentum equation and turbulence model equations. The diffusive terms were

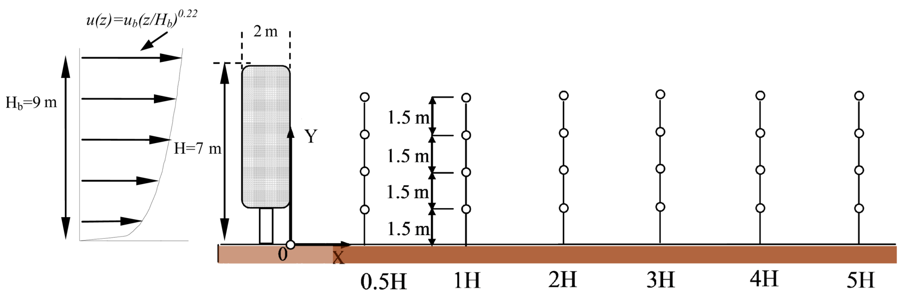

Fig. 1 Scheme of numerical model of windbreak flow (referred to http://www.aij.or.jp/)

discretized by second order central difference scheme. The flow field was initiated by the inlet boundary condition. The convergence criteria of the scaled residuals for all variables and the continuity equation were set as 10^{-4}. To obtain convergent results, although the convergence criteria were achieved, additional iterations were performed to ensure a stable convergence over a sufficient period.

The numerical simulations on different mesh resolutions were performed at the onset to check the requirement of mesh independence. Four variations of mesh densities, which was similar to that was adopted in Yang *et al*. (2009), were investigated. It was concluded that the CFD simulation results under the present settings were independent of the mesh resolution.

3.2 Modeling of equilibrium atmospheric boundary layer

The modeling of equilibrium ABL was an important precondition for a proper numerical simulation of flows around buildings (Blocken *et al*. 2007). The most important requirement of equilibrium ABLs was the horizontal homogeneity, which means that the streamwise gradients of all variables should be zero.

The issue of generating an equilibrium ABL was investigated from the viewpoint of the turbulence model. The approximate solution to the standard k-ε model was derived based on the assumption of the local equilibrium of turbulence, and then a new set of inflow turbulence boundary conditions for modeling equilibrium ABL was proposed (Yang *et al*. 2008, 2009b). The application of the new inflow boundary conditions was further extended to the SST k-ε model for modeling equilibrium ABL (Yang *et al*. 2009a). The performance and applicability of this new set of inflow boundary condition have been recently validated (Gorlé *et al*. 2010, O'Sullivan *et al*. 2011), and it has been adopted in the numerical simulations of ABL transport phenomena (Barić *et al*. 2011,

Table 1 Boundary conditions of the numerical model

Location	Boundary conditions	
Inflow face	Defining the mean velocity (u), TKE (k) and turbulence frequency (ω)	$u = u_b\left(\frac{z}{H_b}\right)^{\alpha}$, $v = 0$, $w = 0$; $k = \sqrt{D_1 z^{\alpha_i} + D_2}$, $\omega = \varepsilon/(C_\mu \cdot k)$; where $\varepsilon = \alpha_i C_\mu^{\frac{1}{2}} \frac{u}{z} \sqrt{D_1 z^{\alpha_i} + D_2}$
Outflow face	Fully developed outflow	$\frac{\partial}{\partial x}(u, v, w, k, \omega) = 0$
Upper face of computational domain	Free slip	$w = 0,\ \frac{\partial}{\partial y}(u, v, k, \omega) = 0$
Side faces of computational domain	Free slip	$v = 0,\ \frac{\partial}{\partial y}(u, w, k, \omega) = 0$
Ground surface boundary	wall	No slip wall with wall roughness modification, roughness height $Ks = 0.05$ m and roughness constant $Cs = 0.5$

Kozmar, 2011, Labovský and Jelemenský 2011).

The first step of the numerical verification was the simulation of simple boundary layer flow in an empty domain to confirm whether the equilibrium ABL is adequately generated. The boundary conditions of the numerical model were defined in Table 1. The parameters in the inflow boundary conditions were referred to the experiment of Kurotani *et al*. (2002) and the numerical simulations by Mochida *et al*. (2006), in which $u = 5.6$ m/s, $H_b = 9$ m, $\alpha = 0.22$, $D_1 = -8.94\ \mathrm{m}^{4-\alpha}/\mathrm{s}^4$, $D_2 = 53.4\ \mathrm{m}^4/\mathrm{s}^4$.

4. Numerical simulation results

4.1 ABL simulation

Fig. 2 illustrates the comparisons of the mean velocity and the turbulent kinetic energy profiles at the inlet, 1/2 L and outlet of an empty domain model. As can be seen from Fig. 2, under the present inflow turbulence boundary conditions, both the mean velocity and turbulent kinetic energy profiles were sustained satisfactorily throughout the whole domain, except for the turbulent kinetic energy profile in the region near the ground surface. The error was attributable to the roughness wall treatment (Yang *et al*. 2008).

4.2 Tree canopy flow

Fig. 3 compares the mean velocity profiles obtained from the current numerical simulation to the experimental data (Kurotani *et al*. 2002) at different locations downstream of the vegetated windbreak. It can be seen from Fig. 3 that the numerical results show considerable agreement with the experimental data in the near wake region, while they were slightly smaller than the experimental results in the far field of wake region. The deviations can probably be attributed to following reasons:

1. The mean velocity profile depends on the parameters designated to the additional source/sink terms. Mochida *et al*. (2006) performed the parameter optimization study and concluded that the numerical results were heavily relied on the choices of the parameters. In the current study, a similar study on the parameters, i.e., α_p and α_d, β_p and β_d, in the additional source/sink terms has

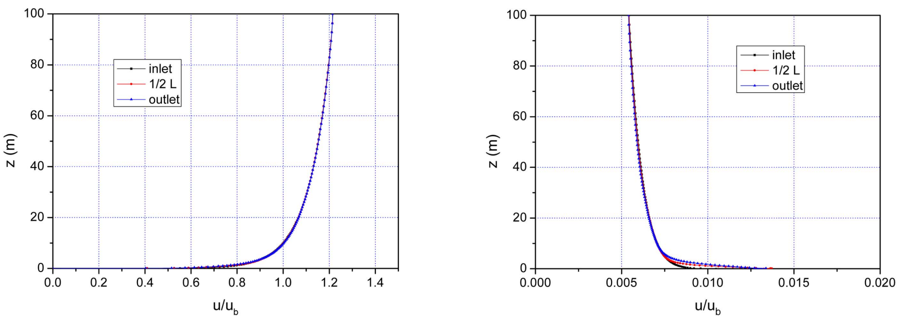

(a) Mean velocity u/u_b (b) Turbulent kinetic energy k/u_b^2

Fig. 2 Comparisons of the mean velocity and the turbulent kinetic energy profiles at the inlet, 1/2 L and outlet (u_b was defined as the inflow velocity at 10 m height)

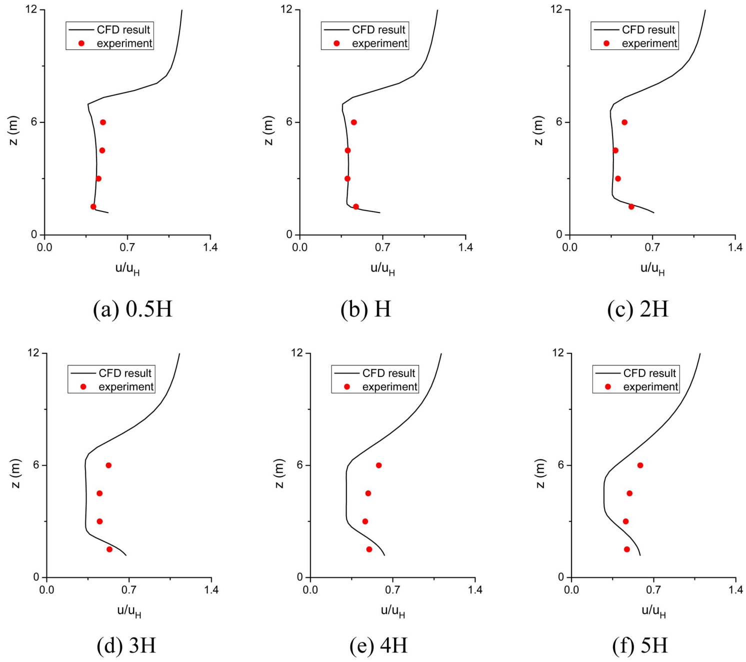

Fig. 3 Comparisons of the mean velocity profiles at different locations downstream of the vegetated windbreak

been carried out to identify the optimal values. It concluded that the parameters used in this paper provide relatively better results.

2. They might be influenced by some differences between the numerical model developed in this paper and the field experiment referred to. For example, some details of the numerical model had to be simplified for only limited information about the tree canopy and its terrain condition being available. Besides, using simplified 2D model to reflect the real 3D flow phenomenon would also affect the numerical accuracy.

Despite of the discrepancy, the verification work of the windbreak flow exhibited the applicability of the presented source/sink term model in simulating the canopy flow. Based on this work, the method would be further applied to the wind environment optimization of the high-rise buildings of China Academy of Building Research (CABR).

5. Application

5.1 Introduction

The assessment and modification research of wind environment of the high-rise buildings Silvertop Towers had been reported by Blocken *et al.* (2004). CFD simulation was demonstrated being an effective method for such assessment (Blocken and Carmeliet 2008).

In this section, twin high-rise buildings of CABR were chosen as an example. The new mansion

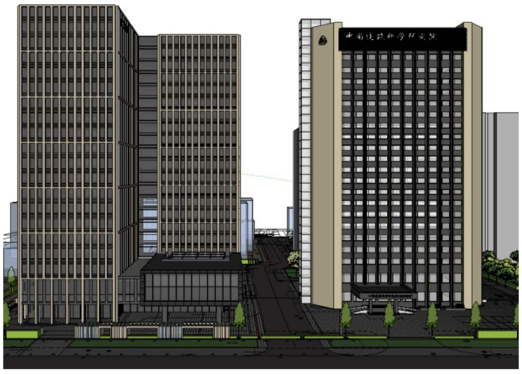

Fig. 4 Scheme of the new building of China Academy of Building Research

of CABR (i.e., the left building in Fig. 4) was built close to the existing building, and both were 80 m in height (h). Due to the limited site area, the minimum width of the passage, b_{min}, is only about 15 m. Therefore, the ratio of b_{min}/h was as small as 0.19. This narrow passage formed by two closely arranged high-rise buildings will be the main entrance of CABR in the future.

Due to lack of obstacles in front of the buildings, moreover, the passage being towards the local dominant wind direction in the whole year, therefore, the pedestrian wind environment was deteriorated in windy days for the wind speed in the passage being accelerated apparently. In order to quantitatively evaluate the pedestrian wind environment comfort and safety around the buildings, particularly at the narrow passage, a detailed wind tunnel test and numerical simulations had been carried out.

According to the wind tunnel test and the numerical simulations, the maximum wind speed ratio C_u, which was defined as the ratio of the local mean wind speed U_p to the undisturbed wind speed U_f at the pedestrian level., i.e., $C_u = U_p/U_f$, could reach 1.8. Combining with the local wind climate statistic data, it resulted that the peak wind speed was as high as the Beaufort scale 8. The probability of occurrence of such high wind speed in the passage was estimated to be nearly 8 times per year. That implied the wind environment in the passage does not satisfy the basic requirements of safety and comfort for pedestrians.

5.2 Wind environment optimization design

In order to ameliorate the unfavorable wind environment, additional optimization scheme in cooperation with architects have been performed. Some remedial measures were suggested, for example, a large billboard as high as 9 m was planned to set up in front of the windward opening of the passage as a windbreak, and the semi-opened corridor on the ground floor of the new mansion was recommended to be closed and used as pedestrian pathway, as depicted in Fig. 5.

Though the proposed measures can potentially ameliorate the high wind speed environment at some extent, further numerical simulation (numerical model see Fig. 6) showed that the wind speed at the pedestrian level still tended to unfavorable. This is because the major characteristic of the narrow passage formed by the two high-rise buildings largely remains unchanged.

For example, the big billboard can successfully block off strong wind from north in the downstream near field but the flow separated over the billboard was speeding up and reattaching farther downstream, as reported in Fig. 7. Therefore the high wind speed environment in the

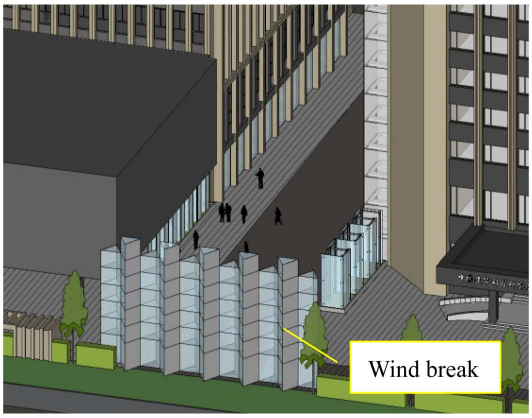

Fig. 5 The optimization measures of alleviating unfavorable wind

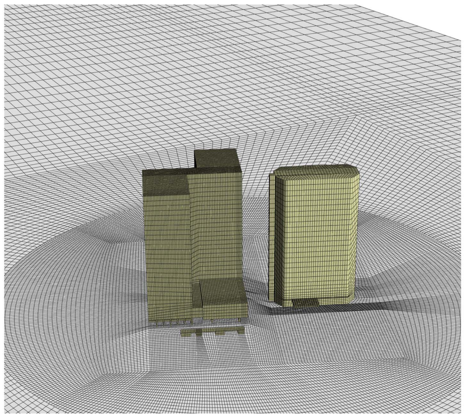

Fig. 6 Grid discretization of the numerical model of CABR buildings

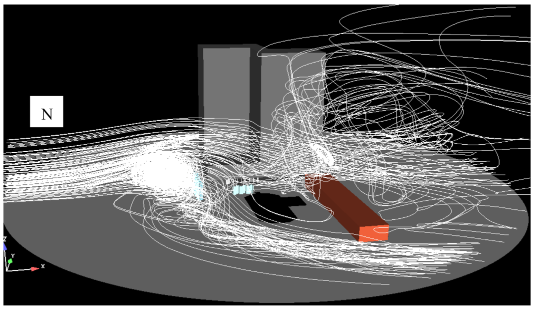

Fig. 7 The wind flow streamlines around the building under the north wind

southern end of the passage was not mitigated and may even be worse in some situations as demonstrated here. Consequently, optimizing the quality of the wind environment around the building, in particular the passage was challenging for wind engineers.

5.3 Application of the tree canopy in the optimization design

5.3.1 Numerical model

The idea of installing tree canopy in the passage acting as a "soft" windbreak was then proposed and the numerical simulation was carried out. The full scale 3D model of CABR buildings was built according to the architectural design. Some unnecessary architectural details and features were simplified to avoid over-weighted calculation load. The dimensions of the computational domain were set as 720 m × 1360 m × 560 m (i.e., W × L × H), resulting in the blockage ratio of the domain being smaller than 3%.

The grid discretization scheme was designed to achieve a balance between the precision of numerical results and the computational time. The whole domain was divided into two parts as showed in Fig. 6 and then hexahedron cells were adopted for both internal and external parts' discretization. The size of the smallest cells close to the building boundaries in the internal part was approximately 0.5 m. This scheme gives the total grid cells of about 2 million.

The boundary conditions were set following the expressions in Tab.1, while the two constants of

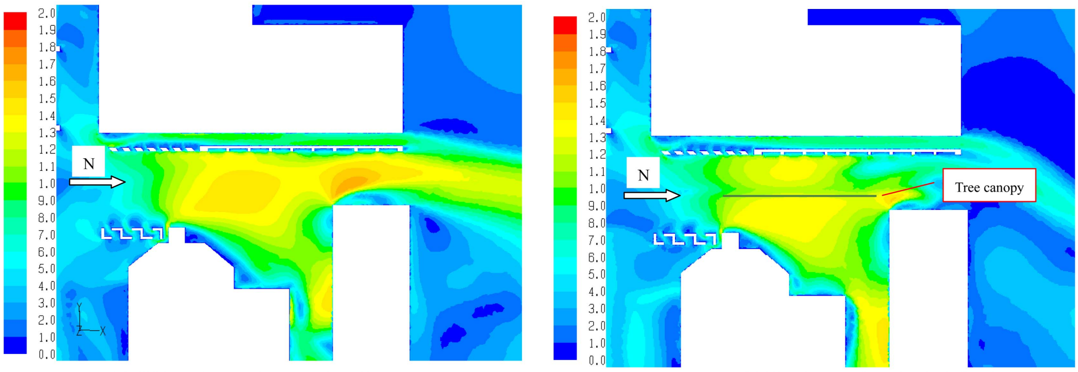

(a) Without the central vegetated windbreak (b) With the central vegetated windbreak

Fig. 8 Comparisons of the contours of the wind velocity ratios *Cu* at the pedestrian level before/after setting the vegetated windbreak in the center of the passage

k, D_1 and D_2 were changed slightly in consideration of the local wind terrain feature. Here they were defined as: $D_1 = -8.93$ m$^{4-\alpha}$/s^4, $D_2 = 53.1$ m^4/s^4; where $\alpha = 0.22$.

In the numerical model, a line of tree canopy was set in the middle of the passage, as illustrated in Fig. 8(b). The dimensions of the tree model were 50.0 m(L) × 1.0 m(W) × 1.5 m(H). The drag coefficient C_d and LAD of the tree model were 0.8 and 1.17 m^2/m^3, respectively. The details of the tree windbreak can be referred to the paper of Kurotani *et al*. (2002).

5.3.2 Calculation results

Fig. 8 illustrates the comparisons of the wind velocity ratios C_u at the pedestrian level before and after setting up the vegetated windbreak in the center of the passage subject to the north wind. It can be clearly seen from Fig. 8(b) that the high wind velocity ratio (i.e., C_u >1.5) was restrained and the area with high wind velocities, especially in the southern part of passage, was reduced significantly after the tree canopy was "planted". Therefore, it could partly overcome the negative influence brought by the installation of the windbreak at the northern end as showed in Fig. 7.

Numerical simulations exhibited the effects of the tree canopy partly eliminating the unfavorable strong pedestrian wind and improving the wind environment in the passage. Based on the numerical results, a proposal of ameliorating the wind environment of this development project was presented. A line of tree canopy in the middle of the passage with properly designed windbreak facilities installed at the northern end of the passage can effectively reduce the high wind speed and avoid the unfavorable wind environment.

6. Conclusions

Existing turbulence models have been improved in order to appropriately consider the effect of tree canopy on the wind environment flow, which is realized by introducing additional source/sink terms in the governing equations. The new source term model S_ω for the turbulence frequency ω equation in the SST k-ω model was derived through the theoretical analogy. Its applicability and performance were numerically verified by performing the simulation of the windbreak flow. Then the proposed source term model was adopted in the wind environment optimal design of the twin high-rise buildings of CABR.

Using the new inflow boundary conditions developed in the previous study to model the equilibrium atmospheric boundary layer, it was concluded that the theoretically reasonable source/sink term model of the SST k-ω model was applicable for the modeling of tree canopy flow. Though some optimization works of the parameters in the model have been performed to achieve better results, the authors believe that more refined study will be helpful for further improving the numerical accuracy.

Acknowledgements

Financial supports of this study from the National Key Technology R&D Program during the 11th Five-Year Plan Period under Grant No. 2006BAJ02A05 and the National Natural Science Foundation of China under Grant No. 50708014, 51178441 are gratefully appreciated. The study reported in this paper is partly carried out under the support of the RGC General Research Fund, HKSAR Project No. 9041338.

References

Bariæ, E., Džijan, I. and Kozmar, H. (2010), "Numerical simulation of wind characteristics in the wake of a rectangular building submitted to realistic boundary layer conditions", *Trans. Famena*, **34**(3), 1-10.

Blocken, B., Stathopoulos, T. and Carmeliet, J. (2007), "CFD simulation of the atmospheric boundary layer: wall function problems", *Atmos. Environ*., **41**(2), 238–252.

Blocken, B., Roels, S. and Carmeliet, J. (2004), "Modification of pedestrian wind comfort in the Silvertop Tower passages by an automatic control system", *J. Wind Eng. Ind. Aerod*., **92**(10), 849-873.

Blocken, B. and Carmeliet, J. (2008), "Pedestrian wind conditions at outdoor platforms in a high-rise apartment building: generic sub-configuration validation, wind comfort assessment and uncertainty issues", *Wind Struct*., **11**(1), 51-70.

Franke, J., Hellsten, A., Schlünzen, H. and Carissimo, B. (2007), *Best practice guideline for the CFD simulation of flows in the urban environment*, COST Office, Brussels, http://www.mi.uni-hamburg.de/Official-Documents.5849.0.html

Gorlé, C., van Beeck, J. and Rambaud, P. (2010), "Dispersion in the wake of a rectangular building: validation of two reynolds-averaged navier-stokes modelling approaches", *Boundary-Lay. Meteorol*., **137**(1), 115-133.

Green, S.R. (1992), "Modelling turbulent air flow in a stand of widely-spaced trees", *Int. J. Comput. Fluid D*., **5**, 294-312.

Kozmar, H. (2011), "Wind-tunnel simulations of the suburban ABL and comparison with international standards", *Wind Struct*., **14**(1), 15-34.

Kurotani Y., Kiyota N. and Kobayashi S. (2002), *Windbreak effect of Tsuijimatsu in Izumo Part 2*, Summaries of technical papers of annual meeting, AIJ Environmental Engineering I (in Japanese), 745–746.

Labovský, J. and Jelemenský, L. (2011), "Verification of CFD pollution dispersion modelling based on experimental data", *J. Loss Prevent.Proc*., **24**(2), 166-177.

Liu, J., Chen, J.M., Black, T.A. and Novak, M.D. (1996), "*E*-ε modelling of turbulent air flow downwind of a model forest edge", *Bound-Lay.Meteorol*., **77**(1), 21-44.

Menter, F.R. (1994), "Two-equation eddy-viscosity turbulence models for engineering applications", *AIAA J*., **32**(8), 1598-1605.

Mochida, A., Yoshino, H., Iwata, T. and Tabata, Y. (2006), "Optimization of tree canopy model for CFD prediction of wind environment at pedestrian level", *Proceedings of the 4th International Symposium of Computational Wind Engineering* , Yokohama, 561-564.

Mochida, A., Tabata, Y., Iwatab, T. and Yoshino, H. (2008), "Examining tree canopy models for CFD prediction of wind environment at pedestrian level", *J. Wind Eng. Ind. Aerod*., **96**(10-11), 1667–1677.

Neary, V.S. (2003), "Numerical solution of fully developed flow with vegetative resistance", *J. Eng. Mech.-ASCE*, **129**(5), 558-563.

Pattanapol, W., Wakes Sarah, J., Hilton Michael, J. and Dickinson Katharine, J.M. (2008), "Modeling of surface roughness for flow over a complex vegetated surface", *J. Math.Phys*., **2**(1), 18-26.

O'Sullivan, J.P., Archer, R.A. and Flay, R.G.J. (2011), "Consistent boundary conditions for flows within the atmospheric boundary layer", *J. Wind Eng. Ind. Aerod*., **99**, 65-77.

Svensson, U. and Haggkvist, K. (1990), "A two-equation turbulence model for canopy flows", *J. Wind Eng. Ind. Aerod*., **35**, 201-211.

Sogachev, A. and Panferov, O. (2006), "Modification of two-equation models to account for plant drag", *Bound-Lay.Meteorol*., **121**(2), 229-266.

Versteeg, H.K. and Malalasekera, W. (1995), *An introduction to computational fluid dynamics: the finite volume method*, Longman Group Ltd, UK.

Yang, W., Quan, Y., Jin, X.Y., Tamura, Y. and Gu, M. (2008), "Influences of equilibrium atmosphere boundary layer and turbulence parameter on wind loads of low-rise building", *J. Wind Eng. Ind. Aerod*., **96**(10-11), 2080-2092.

Yang, Y., Gu, M. and Jin, X.Y. (2009a), "New inflow boundary conditions for modeling the neutral equilibrium atmospheric boundary layer in SST k-ω Model", *Proceedings of the 7th Asia-Pacific Conference on Wind Engineering*, Taipei, Taiwan.

Yang, Y., Gu, M., Chen, S.Q. and Jin, X.Y. (2009b), "New inflow boundary conditions for modeling the neutral equilibrium atmospheric boundary layers in computational wind engineering", *J. Wind Eng. Ind. Aerod*., **97**(2), 88-95.

CC